JACS
JOURNAL OF THE AMERICAN CHEMICAL SOCIETY

Communication

pubs.acs.org/JACS

# Multiple Functionalities of Polyfluorene Grafted with Metal Ion-Intercalated Crown Ether as an Electron Transport Layer for Bulk-Heterojunction Polymer Solar Cells: Optical Interference, Hole Blocking, Interfacial Dipole, and Electron Conduction

Sih-Hao Liao, Yi-Lun Li, Tzu-Hao Jen, Yu-Shan Cheng, and Show-An Chen*

Chemical Engineering Department and Frontier Research Center on Fundamental and Applied Sciences of Matters, National Tsing-Hua University, Hsinchu 30013, Taiwan, ROC

Supporting Information

**ABSTRACT:** We present a novel electron transport (ET) polymer composed of polyfluorene grafted with a $K^+$-intercalated crown ether involving six oxygen atoms (PFCn6:$K^+$) for bulk-heterojunction polymer solar cells (PSCs) with regioregular poly(3-hexylthiophene) (P3HT) as the donor and indene−$C_{60}$ bisadduct (ICBA) or indene−[6,6]-phenyl-$C_{61}$-butyric acid methyl ester (IPCBM) as the acceptor in the active layer and with Al or Ca/Al as the cathode. A remarkable improvement in the power conversion efficiency (PCE) (measured in air) was observed upon insertion of this ET layer, which increased the PCE from 5.78 to 7.5% for a PSC with ICBA and Ca/Al (5.53 to 6.63% with IPCBM) and from 3.87 to 6.88% for a PSC with ICBA and Al (3.06 to 6.21% with IPCBM). This ET layer provides multiple functionalities: (1) it generates an optical interference effect for redistribution of light intensity as an optical spacer; (2) it blocks electron−hole recombination at the interface with the cathode; (3) it forms an interfacial dipole that promotes the vacuum level of the cathode metal; and (4) it enhances electron conduction, as evidenced by (1) the increase in total absorption of 1:1 w/w P3HT:ICBA by a factor of 1.3; (2) the reduction in the hole-only current density profile by a factor of 3.3 at $2.0 \times 10^5$ V/cm; (3) the decrease of 0.81 eV in the work function of Al from 4.28 to 3.47 eV, as determined by UV photoelectron spectroscopy; and (4) the decrease in the series resistance of PSCs with ICBA and Al by a factor of 4.5, as determined by the current−voltage characteristic under dark conditions; respectively. The PSC of 7.5% is the highest among the reported values for PSC systems with the simplest donor polymer, P3HT.

Bulk-heterojunction (BHJ) polymer solar cells (PSCs)[1] with an active layer composed of a conjugated polymer as the donor and a fullerene derivative as the acceptor have attracted great attention because of their ease of fabrication, promising flexibility, and capability for large-scale and low-cost production. Poly(3-hexylthiophene) (P3HT) with high regioregularity and [6,6]-phenyl-$C_{61}$-butyric acid methyl ester (PCBM) are the most representative conjugated polymer donor material and acceptor material, respectively. PSCs based on these two materials can reach the power conversion efficiencies (PCEs) of 4−5%.[2] The limited performance is due to the low open-circuit voltage ($V_{oc}$)[3] of 0.5−0.7 V resulting from the low energy of the lowest unoccupied molecular orbital (LUMO) of PCBM (−3.91 eV), as $V_{oc}$ depends on the difference between the LUMO energy of the acceptor and the highest occupied MO (HOMO) energy of the donor.[4] To enhance the PCE by design of the active layer, one way is to design an acceptor with a higher LUMO energy, increasing $V_{oc}$. Some fullerene derivatives have been reported to give higher $V_{oc}$ because of their higher LUMO energies, such as PCBM bisadduct[5] ($E_{LUMO}$ = −3.7 eV, $V_{oc}$ = 0.724 V), indene−PCBM[6] (IPCBM) ($E_{LUMO}$ = −3.79 eV, $V_{oc}$ = 0.72 V), and indene−$C_{60}$ bisadduct (ICBA) ($E_{LUMO}$ = −3.74 eV, $V_{oc}$ = 0.84 V). ICBA provided the highest reported PCE with P3HT (6.48%).[7] The other way is to replace P3HT with lower-band-gap polymers, allowing the promotion of the PCE from 5 to over 7%, as reported for PSCs with donors such as thieno[3,4-*b*]thiophene/benzodithiophene (PTB7) and poly[*N*-9″-heptadecanyl-2,7-carbazole-*alt*-5,5-(4′,7′-di-2-thienyl-2′,1′,3′-benzothiadiazole)] (PCDTBT) along with fullerene derivative acceptors such as [6,6]-phenyl-$C_{71}$-butyric acid methyl ester ($PC_{71}BM$) and PCBM.[8−11]

Other than material design for the active layer, the insertion of an electron transport layer (ETL) between the active layer and the metal cathode can also increase the PCE. For example, water- or alcohol-soluble ETLs based on conjugated polyfluorene grafted with *N*,*N*-dimethylamino (PFN),[12] ammonium salt (WPF-oxy),[13] or phosphonate (PF−EP)[14] have been used in P3HT:PCBM systems with Al as the cathode, giving PCE enhancements of 0.08% (from 1.42 to 1.54%), 0.82% (from 2.95 to 3.77%), and 1.4% (from 1.98 to 3.38%), respectively. It was recently found that the PCE can be enhanced from 5 to 6.5% via insertion of an interlayer consisting of a conjugated polymer grafted with ammonium salt (PF2/6-*b*-P3TMAHT) between the PCDTBT:$PC_{71}BM$ active layer and the Al cathode.[15] Also, the incorporation of PFN as an interlayer inserted between the active layer [composed of quinoxaline-containing poly(4,5-ethylene-2,7-carbazole) (PECz−DTQx), PCDTBT, or PTB7 as the donor and $PC_{71}BM$ as the acceptor] and the cathode (Al or Ca/Al) was found to improve the PCE from 3.99 to 6.07% for the first donor (Al cathode),[16] 4.11 to 6.79% for the second donor (Ca/Al cathode),[17] and 7.13 to 8.37% for the third donor (Ca/Al

**Received:** April 20, 2012
**Published:** August 17, 2012

cathode).[17] The improvements were attributed to better interfacial contact with the Ca/Al cathode and the formation of an interfacial dipole[17] of PFN with the positively charged end pointing toward the Al cathode.

Here we employed as ETLs novel polymers composed of polyfluorene grafted with $K^+$-intercalated crown ethers involving six, five, or four oxygen atoms, designated as PFCn6:$K^+$ (Scheme 1a), PFCn5:$K^+$, and PFCn4:$K^+$, respectively, which are soluble in

**Scheme 1. (a) Chelation of PFCn6 to $K^+$; (b) Schematic Illustration of the Proposed Working Mechanism[a]**

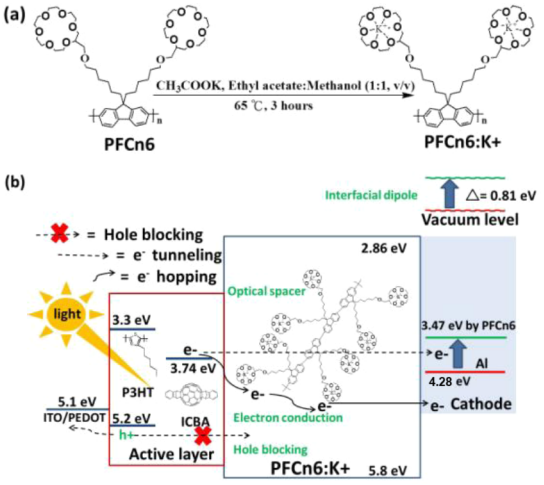


[a]In (b), the labels on the energy levels are the corresponding energies multiplied by −1,[7a,18] and Δ denotes the shift in the vacuum level.

ethyl acetate/alcohol mixed solvent. The ET polymer provides multiple functionalities: (1) it generates an optical interference effect for redistribution of light intensity as an optical spacer; (2) it blocks electron−hole recombination at the interface with the cathode; (3) it forms an interfacial dipole that promotes the vacuum level of the cathode metal; and (4) it enhances the electron conductivity. Scheme 1b shows the working mechanism for this ETL. Although these polymers have been successfully used by us as electron injection layers for high-performance deep-blue-emitting polymer light-emitting diode (PLEDs)[18] with Al as the cathode, here they provide functionalities different from those in PLEDs and work remarkably well in PSCs with an active layer composed of P3HT as the donor material and ICBA or IPCBM as the acceptor material [chemical structures for all of the materials used are shown in Chart S1 in the Supporting Information (SI)]. Among the three intercalated ET polymers, PFCn6:$K^+$ is the best one, permitting an improvement in the PCE with ICBA from 5.78 to 7.50% (measured in air), which is the highest among the values reported for PSCs with the simplest donor polymer, P3HT. Those next to it are 6.69% for P3HT:$IC_{70}BM$ with Ca as the cathode along with the addition of methylthiophene but without an ETL[19] and 7.3% for an inverted PSC of P3HT:ICBA with ZnO as the cathode and cross-linked fullerene rods (C-PCBSD)[20] as the ETL. For PSCs with IPCBM instead of ICBA, the PFCn6:$K^+$ ETL also improved the PCE from 5.53 to 6.63%.

Figure 1 presents current density versus applied voltage ($J$−$V$) curves and external quantum efficiency (EQE) spectra of the devices ITO/PEDOT:PSS (25 nm)/P3HT:ICBA (1:1 w/w, 180 nm)/ETL (5 nm or none)/cathode (Al or Ca/Al) under simulated 100 mW/cm$^2$ AM 1.5G illumination, and their

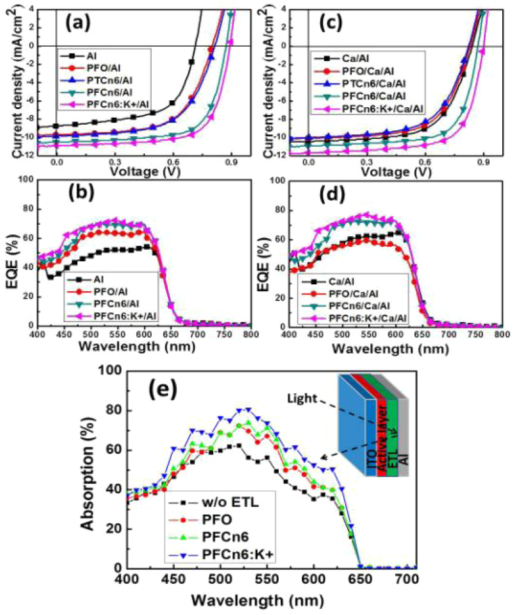


**Figure 1.** Performance of PSCs under simulated 100 mW/cm$^2$ AM 1.5G illumination. (a) $J$−$V$ curves and (b) EQE spectra of the devices ITO/PEDOT:PSS (25 nm)/P3HT:ICBA (1:1 w/w, 180 nm)/ ETL (5 nm or none)/Al (100 nm). (c) $J$−$V$ curves and (d) EQE spectra of the devices identical to those in (a) and (b) except with a Ca/Al cathode. (e) Total absorption spectra in similar devices with the Al cathode but without the hole transport layer (PEDOT:PSS), measured in the reflection geometry. The inset shows the device structure.

characteristic values are listed in Table 1. An investigation of the effect of the thickness of the ETL on the performance by varying it from 5 to 20 nm for all the devices showed that thinner ETLs were better in all cases (Figures S2−S5 and Table S2 in the SI). For the devices with Al and ICBA, use of PFCn6 as the ETL gave remarkably increased performance relative to that for the

**Table 1. Performance of PSCs with or without an ETL[a]**

| acceptor, cathode | ETL | $V_{oc}$ (V) | $J_{sc}$ (mA/cm$^2$) | FF (%) | PCE (%) |
|---|---|---|---|---|---|
| ICBA, Al | none | 0.71 | 8.74 | 62.4 | 3.87 |
| ICBA, Al | PFCn6 | 0.87 | 10.53 | 69.4 | 6.35 |
| ICBA, Al | PFCn6:$K^+$ [b] | 0.89 | 10.96 | 70.6 | 6.88 |
| ICBA, Al | PFO | 0.81 | 9.67 | 65.2 | 5.10 |
| ICBA, Al | PEO | 0.74 | 7.41 | 50.0 | 2.74 |
| ICBA, Al | PTCn6 | 0.81 | 9.84 | 61.6 | 4.90 |
| ICBA, Ca/Al | none | 0.85 | 10.43 | 65.2 | 5.78 |
| ICBA, Ca/Al | PFCn6 | 0.87 | 10.93 | 71.2 | 6.77 |
| ICBA, Ca/Al | PFCn6:$K^+$ [b] | 0.89 | 11.65 | 72.6 | 7.50 |
| ICBA, Ca/Al | PFCn5:$K^+$ [b] | 0.88 | 11.33 | 71.2 | 7.10 |
| ICBA, Ca/Al | PFCn4:$K^+$ [b] | 0.87 | 11.12 | 69.5 | 6.72 |
| ICBA, Ca/Al | PFO | 0.83 | 10.02 | 64.3 | 5.34 |
| ICBA, Ca/Al | PEO | 0.82 | 8.81 | 65.2 | 4.71 |
| ICBA, Ca/Al | PTCn6 | 0.82 | 9.97 | 62.5 | 5.10 |
| IPCBM, Al | none | 0.68 | 7.12 | 63.4 | 3.06 |
| IPCBM, Al | PFCn6 | 0.83 | 10.43 | 68.9 | 5.96 |
| IPCBM, Al | PFCn6:$K^+$ [b] | 0.85 | 11.21 | 65.2 | 6.21 |
| IPCBM, Ca/Al | none | 0.80 | 10.12 | 68.4 | 5.53 |
| IPCBM, Ca/Al | PFCn6 | 0.85 | 10.78 | 70.5 | 6.45 |
| IPCBM, Ca/Al | PFCn6:$K^+$ [b] | 0.86 | 10.93 | 70.6 | 6.63 |

[a]Device structure: ITO/PEDOT:PSS (25 nm)/P3HT:acceptor (1:1 w/w, 180 nm)/ETL (5 nm or none)/cathode. [b]1:1 mole ratio.


dx.doi.org/10.1021/ja303813s | J. Am. Chem. Soc. 2012, 134, 14271−14274

device with no ETL, as the PCE increased from 3.87 to 6.35% and all the three corresponding parameters [$V_{oc}$, the short-circuit current density ($J_{sc}$), and the fill factor (FF)] were improved from 0.71 V, 8.74 mA/cm$^2$, and 62.4%, respectively, to 0.87 V, 10.53 mA/cm$^2$, and 69.4%, respectively. The improvement in $V_{oc}$ and $J_{sc}$ can be attributed mainly to light intensity redistribution (allowing more effective absorption of sunlight), the presence of the interfacial dipole (causing a rise in the vacuum level of the Al cathode), and hole blocking along with a minor contribution from exciton blocking provided by the insertion of the ETL, as revealed by the following results. With PFCn6, the EQEs from 450 to 625 nm are in the range 60−70%, which are much higher than those without the ETL (40−55%) (Figure 1b); this is in agreement with the higher $J_{sc}$ mentioned above. To investigate the origin of the photocurrent improvement, we measured the optical interference (or optical spacer) effect in accordance with the reported procedure[8] and the exciton blocking effect by time-resolved photoluminescence (PL). The presence of the optical interference effect is manifested in the reflectance spectra by the promoted absorption profile of the active layer in the range 450−650 nm with a slight red shift of ∼10 nm for the device ITO/P3HT:ICBA (1:1 w/w, 180 nm)/ETL (5 nm)/Al (100 nm) compared with that without the ETL (Figure 1e). More specifically, for P3HT:ICBA (1:1 w/w) devices with PFCn6 and poly(9,9-di-*n*-octylfluorene) (PFO) ETLs, the ratio of the areas under the absorption curves was promoted by factors of 1.17 and 1.12, respectively, and the ratio of the absorption maxima by factors of 1.31 and 1.23, respectively, relative to those for the device without this layer (Table S8), indicating that the PF main chains in the ETL do provide a 12% enhancement in absorption by redistribution of light intensity and that the grafted crown ether moieties give only a minor enhancement (5% more). Since the HOMO and LUMO levels of the ETL cover those of P3HT, one may expect an exciton blocking effect for the active layer. However, the number of generated excitons that are able to diffuse toward the cathode is limited because the singlet exciton lifetime decays from 850 ps to 16−5 ps as 5−50 wt % PCBM is added[21] (see section S4 in the SI for details). Even though the ETL−active layer interfacial region might have smaller ICBA content, as in the case of P3HT:PCBM (1:1 w/w) in which the average content of PCBM within 20 nm of the interfacial region is reduced to 22%,[22] the number of excitons generated in this region (13% of the total thickness) that are able to diffuse to the surface before being dissociated by ET to ICBA is still limited. Therefore, the contribution to the promoted photocurrent from exciton blocking by the ETL is secondary relative to that of the optical interference effect. Since the ETL's HOMO (−5.8 eV) is 0.6 eV lower than that of P3HT (−5.2 eV), we would expect a hole blocking effect, which was confirmed by the measurement of the hole-only current density versus electric field for the devices without and with the PFCn6 ETL (Figure S15). The hole current density profiles were reduced significantly (e.g., by a factor of 3.6 at 2.0 × 10$^5$ V/cm) relative to that without the ETL. Thus, the ETL also provides a significant hole blocking effect.

For the interfacial dipole effect provided by PFCn6 (PFO) on the Al cathode, as measured using UV photoelectron spectroscopy (UPS), the vacuum level of Al was found to rise by 0.81 (0.76) eV (Figure S1 and Table S1) relative to that of bare Al (−4.28 eV), allowing electrons to be collected by the Al cathode more easily. This indicates that in addition to the polyfluorene main chain, the crown ether moiety in the former also contributes to the interfacial dipole, although by only 0.05 eV (see section S3 for details). To verify the contribution of the crown ether moiety to the PSC performance, we also measured the performance of the device in which PFCn6 was replaced with PFO (Table 1). The small additional dipole moment of the crown ether provided enhancements of 0.06 V in $V_{oc}$, 0.86 mA/cm$^2$ in $J_{sc}$, and 4.2% in FF, resulting in a significant increase of 1.25% in the PCE. In addition to dipole contributions by PFO and PFCn6, electron conductivity provided by the semiconducting polyfluorene main chain is also important, as supported by the drop in performance for the device with a thin (5 nm) layer of the insulating polymer poly(ethylene oxide) (PEO) as the ETL ($J_{sc}$ dropped by 1.33 mA/cm$^2$, FF by 12.4%, and PCE by 1.13%), although a slight dipole contribution of 0.03 V to $V_{oc}$ was observed (Table 1).

We further modified the PFCn6 ETL above by intercalating $K^+$ ions into its crown ether moieties. This gave further appreciable improvements in all the three performance parameters, increasing the PCE by 0.53%. Such improvement mainly resulted from further promotion of the optical interference effect and electron conduction, as revealed below, whereas the additional contribution to the interfacial dipole was insignificant since $V_{oc}$ increased by only 0.02 V. Moreover, the extent of hole blocking decreased slightly (at 2 × 10$^5$ V/cm, the hole current density dropped by a factor of 3.3, which is less than the factor of 3.6 for PFCn6, as shown in Figure S15). Surprisingly, the intercalated $K^+$ ions provided a remarkable enhancement in the total absorption, as manifested by the increases in the ratio of the areas under the absorption curves and the ratio of absorption maxima of P3HT:ICBA (1:1 w/w) (530 nm) from 1.17 to 1.3 and 1.31 to 1.43 (Figure 1e and Table S8). This indicates that a strong optical interference effect was further provided by the intercalated $K^+$. PFCn6:$K^+$ is believed to be the first case of a polymer optical spacer. The additional electron conduction enhancement can be manifested by calculations of the series resistance ($R_s$) and shunt resistance ($R_{sh}$) from the reciprocals of the slopes of the $J-V$ curves under dark conditions at $I = 0$ and $V = 0$.[23] For the devices without and with PFCn6 and PFCn6:$K^+$, these calculations showed a significant drop in $R_s$ from 18.69 to 6.56 and 4.13 Ω cm$^2$, respectively, and a drastic rise in $R_{sh}$ from 234 to 780 and 1024 Ω cm$^2$, respectively (Figure S6 and Table S3). In addition, we also measured $R_s$ from impedance in the dark under a bias of 0.8 V. For the devices without and with PFCn6 and PFCn6:$K^+$, these measurements also showed a drop in $R_s$ from 38.39 to 33.54 and 29.98 Ω (Figure S14 and Table S7). Furthermore, we also measured the conductivities for PFCn6 with and without $K^+$ intercalation using the four-point probe method and found that the conductivity increased from 7.6 × 10$^{-3}$ to 2.5 × 10$^{-2}$ S/cm after the intercalation (Table S6). These data indicate that the incorporation of the ETL does not increase $R_s$ but actually reduces it; the intercalation of $K^+$ further promotes the electron conductivity. In the meantime, $R_{sh}$ is increased because of reduced leak current, even for the case of the crown ether with the intercalated $K^+$ ions.

Since the morphology of the bicontinuous phases of donor and acceptor components in the active layer is desirable for BHJ PSCs and the crown ether and polyfluorene main chain in PFCn6 and PFCn6:$K^+$ can also form two phases, we used atomic force microscopy in tapping mode to investigate their morphology, as shown in Figure S12. The surface topographical image of P3HT:ICBA shows a fine phase separation and bicontinuous network morphology, and that of PFCn6 shows an islandlike morphology that becomes enhanced after $K^+$ intercalation (see section S5 for details).


dx.doi.org/10.1021/ja303813s | J. Am. Chem. Soc. 2012, 134, 14271−14274

For better electrical contact of the ETL with the cathode, a thin layer (5 nm) of Ca was inserted, giving the device structure ITO/PEDOT:PSS/P3HT:ICBA/ETL (5 nm or none)/Ca/Al. As shown in Figure 1c and Table 1, the trend in the improvement in performance due to insertion of the ETL was similar to that with Al alone as the cathode, but the interfacial dipole contribution to the low-work-function Ca cathode was weaker, as expected.[17] The incorporation of PFCn6 gave slight increases of 0.02 V in $V_{oc}$ (from 0.85 to 0.87 V), 0.5 mA/cm$^2$ in $J_{sc}$ (from 10.43 to 10.93 mA/cm$^2$), and 6% in FF (from 65.2 to 71.2%), consequently increasing the PCE by ∼1%. But in the case of the lower-band-gap ETL (PTCn6) with the same main chain as P3HT, the device with PTCn6 gave a PCE of 5.10%, which is 0.68% lower than that without PTCn6 (Table 1), since it also absorbs light in the same range as P3HT and cannot be used as an optical spacer and exciton blocking layer for a PSC with P3HT. Thus, the optical interference effect given by PFCn6 is confirmed. Furthermore, intercalation of $K^+$ into the crown ether additionally increased $V_{oc}$ slightly by 0.02 V, $J_{sc}$ by 0.72 mA/cm$^2$, and FF by 1.4%, consequently increasing the PCE by 0.73% to a value of 7.5%, which is significantly higher than that without the ETL (5.78%). This PCE of 7.5% is the highest among those published for PSCs with P3HT as the donor. The EQE values with PFCn6 and PFCn6:$K^+$ from 450 to 625 nm are over 70%, much higher than that with PFO (50−55%) and without (50−60%) (Figure 1d); this is in agreement with higher $J_{sc}$ mentioned above.

Other than the insertion of PFCn6:$K^+$, we also prepared PFCn4:$K^+$ and PFCn5:$K^+$ for use as ETLs in devices with Ca/Al. The $J-V$ curves are given in Figure S7, and their characteristic parameters are listed in Table 1. All of the parameters for these devices are significantly higher than those for devices without an ETL, and the performance decreased in the order PFCn6:$K^+$ > PFCn5:$K^+$ >PFCn4:$K^+$ (see section S6 for details).

Besides ICBA, we also investigated another disubstituted fullerene derivative, IPCBM, as the acceptor for the same ETL system with Al or Ca/Al as the cathode. The $J-V$ curves are given in Figure S8, and their performance parameters are listed in Table 1. The trends for improvement due to incorporation of PFCn6 and PFCn6:$K^+$ for the devices with Al and Ca/Al cathodes were similar to those for the corresponding devices with ICBA. For the devices with Al, the PCE improved from 3.06 to 5.96 and 6.21% upon incorporation of PFCn6 and PFCn6:$K^+$, respectively, while for the devices with Ca/Al, the PCE improved from 5.53 to 6.45 and 6.63%, respectively.

In conclusion, we have presented the use of polyfluorene grafted with a crown ether intercalated with $K^+$ (PFCn6:$K^+$) as the electron transport layer in BHJ PSCs with an active layer composed of P3HT as the donor and the disubstituted fullerene ICBA as the acceptor. This led to an improvement in the PCE from 3.87 to 6.88% for the device with Al as the cathode and from 5.78 to 7.50% for that with Ca/Al as the cathode. Similar trends in improvement were observed when ICBA was replaced with IPCBM, but the enhancement was lower by about 0.7−0.9%. The improvement due to PFCn6:$K^+$ results from its multiple functionalities of optical interference (by the intercalated metal ions and the polyfluorene main chain), hole blocking and formation of an interfacial dipole (by the polyfluorene main chains and the crown ether), and enhanced electron conduction (by the intercalated metal ions).

## ■ ASSOCIATED CONTENT

### Supporting Information

Experimental procedures and additional data. This material is available free of charge via the Internet at http://pubs.acs.org.

## ■ AUTHOR INFORMATION


### Corresponding Author

sachen@che.nthu.edu.tw


### Notes

The authors declare no competing financial interest.

## ■ ACKNOWLEDGMENTS

We thank the National Science Council for financial support (NSC 99-2120-M-007-012 and NSC 100-2120-M-007-009).

## ■ REFERENCES


(1) Yu, G.; Gao, J.; Hummelen, J. C.; Wudl, F.; Heeger, A. J. *Science* **1995**, *270*, 1789.

(2) Ma, W.; Yang, C.; Gong, X.; Lee, K.; Heeger, A. J. *Adv. Funct. Mater.* **2005**, *15*, 1617.

(3) Reyes-Reyes, M.; Kim, K.; Carroll, D. L. *Appl. Phys. Lett.* **2005**, *87*, No. 083506.

(4) Brabec, C. J.; Cravino, A.; Meissner, D.; Sariciftci, N. S.; Fromherz, T.; Rispens, M. T.; Sanchez, L.; Hummelen, J. C. *Adv. Funct. Mater.* **2001**, *11*, 374.

(5) Lenes, M.; Wetzelaer, G. J. A. H.; Kooist, F. B.; Veenstra, S. C.; Hummelen, J. C.; Blom, P. W. M. *Adv. Mater.* **2008**, *20*, 2116.

(6) He, Y.; Peng, B.; Zhao, G.; Zou, Y.; Li, Y. *J. Phys. Chem. C* **2011**, *115*, 4340.

(7) (a) He, Y.; Chen, H.-Y.; Hou, J.; Li, Y. *J. Am. Chem. Soc.* **2010**, *132*, 1377. (b) Zhao, G.; He, Y.; Li, Y. *Adv. Mater.* **2010**, *22*, 4355.

(8) (a) Park, S. H.; Roy, A.; Beaupre, S.; Cho, S.; Coates, N.; Moon, J. S.; Moses, D.; Leclerc, M.; Lee, K.; Heeger, A. J. *Nat. Photonics* **2009**, *3*, 297. (b) Kim, J. Y.; Kim, S. H.; Lee, H.-H.; Lee, K.; Ma, W.; Gong, X.; Heeger, A. J. *Adv. Mater.* **2006**, *18*, 572.

(9) Liang, Y.; Wu, Y.; Feng, D.; Tsai, S.-T.; Son, H.-J.; Li, G.; Yu, L. *J. Am. Chem. Soc.* **2009**, *131*, 56.

(10) Chen, H. Y.; Hou, J. H.; Zhang, S. Q.; Liang, Y. Y.; Yang, G. W.; Yang, Y.; Yu, L. P.; Wu, Y.; Li, G. *Nat. Photonics* **2009**, *3*, 649.

(11) Liang, Y.; Xu, Z.; Xia, J.; Tsai, S. T.; Wu, Y.; Li, G.; Ray, C.; Yu, L. *Adv. Mater.* **2010**, *22*, 1.

(12) He, C.; Zhong, C.; Wu, H. B.; Yang, R.; Huang, F.; Bazan, G. C.; Cao, Y. *J. Mater. Chem.* **2010**, *20*, 2617.

(13) Na, S. I.; Oh, S. H.; Kim, S. S.; Kim, D. Y. *Org. Electron.* **2009**, *10*, 496.

(14) Zhao, Y.; Xie, Z. Y.; Qin, C. J.; Qu, Y.; Geng, Y. H.; Wang, L. X. *Sol. Energy Mater. Sol. Cells* **2009**, *93*, 604.

(15) Seo, J.; Gutacker, A.; Sun, Y. M.; Wu, H. B.; Huang, F.; Cao, Y.; Scherf, U.; Heeger, A. J.; Bazan, G. C. *J. Am. Chem. Soc.* **2011**, *133*, 8416.

(16) He, Z. C.; Zhang, C.; Xu, X. F.; Zhang, L. J.; Huang, L.; Chen, J. W.; Wu, H. B.; Cao, Y. *Adv. Mater.* **2011**, *23*, 3086.

(17) He, Z. C.; Zhang, C.; Huang, X.; Wong, W.-Y.; Wu, H. B.; Chen, L. W.; Su, S. J.; Cao, Y. *Adv. Mater.* **2011**, *23*, 4636.

(18) Lu, H.-H.; Ma, Y.-S.; Yang, N.-J.; Lin, G.-H.; Wu, Y.-C.; Chen, S. A. *J. Am. Chem. Soc.* **2011**, *133*, 9634.

(19) Sun, Y.; Cui, C.; Wang, H.; Li, Y. *Adv. Energy. Mater.* **2011**, *1*, 1058.

(20) Chang, C.-Y.; Wu, C.-E.; Chen, S.-Y.; Cui, C.; Cheng, Y.-J.; Hsu, C.-S.; Wang, Y.-L.; Li, Y. *Angew. Chem., Int. Ed.* **2011**, *50*, 9386.

(21) Guo, J.; Ohkita, H.; Benten, H.; Ito, S. *J. Am. Chem. Soc.* **2010**, *132*, 6154.

(22) Yu, B.-Y.; Lin, W.-C.; Wang, W.-B.; Iida, S.-i.; Chen, S.-Z.; Liu, C.-Y.; Kuo, C.-H.; Lee, S.-H.; Kao, W.-L.; Yen, G.-J.; You, Y.-W.; Liu, C.-P.; Jou, J.-H.; Shyue, J.-J *ACS Nano* **2010**, *4*, 833.

(23) Moliton, A.; Nunzi, J.-M. *Polym. Int.* **2006**, *55*, 583.